

Invited Paper

Discrete breathers in a nutshell

Sergej Flach^{1 a)}¹ *Max-Planck-Institut für Physik komplexer Systeme, Nöthnitzer Str. 38, 01187 Dresden, Germany*^{a)} *flach@pks.mpg.de*

Received April 14, 2011; Revised July 21, 2011; Published January 00, 2012

Abstract: I give a nutshell introduction to the exciting field of discrete breathers / intrinsic localized modes. I focus on how to obtain these states, how they are localized in space, and how they may interact with extended plane wave states. This work is dedicated to Shozo Takeno, one of the early pioneers in the field.

Key Words: intrinsic localized modes, discrete breathers, localization

1. Introduction

In solid-state physics, the phenomenon of localization is usually perceived as arising from extrinsic disorder that breaks the discrete translational invariance of the perfect crystal lattice. Familiar examples include the localized vibrational modes around impurities or defects in crystals and Anderson localization of waves in disordered media [1]. The usual perception among solid-state researchers is that, in perfect lattices excitations must be extended objects as well, essentially plane wave like. Such firmly entrenched perceptions were severely jolted by Ovchinnikov, Takeno and Sievers since the discovery of intrinsic localized modes (ILM) [2, 3], also known as discrete breathers (DB) [4–6]. These states are typical excitations in perfectly periodic but strongly nonlinear systems, and are characterized by being spatially localized, at variance to plane wave states [7–10].

DB-like excitations, being generic objects, have been observed in a large variety of lattice systems that include bond excitations in molecules, lattice vibrations and spin excitations in solids, charge flow in coupled Josephson junctions, light propagation in interacting optical waveguides, cantilever vibrations in micromechanical arrays, cold atom dynamics in Bose-Einstein condensates loaded on optical lattices, among others. They have been extensively studied, and a high level of understanding about their properties has been reached.

Two decades of intensive research have polished our theoretical understanding of DBs in classical nonlinear lattices. The application of the DB concept to quantum lattices, and the contribution of DBs to thermal equilibrium properties including transport, and to the relaxation of complex systems from a nonequilibrium state back to equilibrium, is less intense explored. This work is intended to give a short introduction into the main concepts, and to formulate directions of possible future research in this exciting field.

2. Constructing discrete breathers

Let us study the combined effect of nonlinearity and discreteness on the spatial localization of a discrete breather. For that we look into the dynamics of a one-dimensional chain of interacting

(scalar) oscillators with the Hamiltonian

$$H = \sum_n \left[\frac{1}{2} p_n^2 + V(x_n) + W(x_n - x_{n-1}) \right]. \quad (1)$$

The integer n marks the lattice site number of a possibly infinite chain, and x_n and p_n are the canonically conjugated coordinate and momentum of a degree of freedom associated with site number n . The on-site potential V and the interaction potential W satisfy $V'(0) = W'(0) = 0$, $V''(0), W''(0) \geq 0$. This choice ensures that the classical ground state $x_n = p_n = 0$ is a minimum of the energy H . The equations of motion read

$$\dot{x}_n = p_n, \quad \dot{p}_n = -V'(x_n) - W'(x_n - x_{n-1}) + W'(x_{n+1} - x_n). \quad (2)$$

Let us linearize the equations of motion around the classical ground state. We obtain a set of linear coupled differential equations with solutions being small amplitude plane waves:

$$x_n(t) \sim e^{i(\omega_q t - qn)}, \quad \omega_q^2 = V''(0) + 4W''(0) \sin^2\left(\frac{q}{2}\right). \quad (3)$$

These waves are characterized by a wave number q and a corresponding frequency ω_q . All allowed plane wave frequencies fill a part of the real axis which is coined linear spectrum. Due to the underlying lattice the frequency ω_q depends periodically on q and its absolute value has always a *finite upper bound*. The maximum (Debye) frequency of small amplitude waves $\omega_\pi = \sqrt{V''(0) + 4W''(0)}$. Depending on the choice of the potential $V(x)$, ω_q can be either acoustic- or optic-like, $V''(0) = 0$ and $V''(0) \neq 0$, respectively. In the first case the linear spectrum covers the interval $-\omega_\pi \leq \omega_q \leq \omega_\pi$ which includes $\omega_{q=0} = 0$. In the latter case an additional (finite) gap opens for $|\omega_q|$ below the value $\omega_0 = \sqrt{V''(0)}$.

For large amplitude excitations the linearization of the equations of motion is not correct anymore. Similar to the case of a single anharmonic oscillator, the frequency of possible time-periodic excitations will depend on the amplitude of the excitation, and thus may be located outside the linear spectrum. Let us assume that a time-periodic and spatially localized state, i.e. a *discrete breather*, $\hat{x}_n(t + T_b) = \hat{x}_n(t)$ exists as an exact solution of Eqs. (2) with the period $T_b = 2\pi/\Omega_b$. Due to its time periodicity, we can expand $\hat{x}_n(t)$ into a Fourier series

$$\hat{x}_n(t) = \sum_k A_{kn} e^{ik\Omega_b t}. \quad (4)$$

The Fourier coefficients are by assumption also localized in space

$$A_{k,|n| \rightarrow \infty} \rightarrow 0. \quad (5)$$

Inserting this ansatz into the equations of motion (2) and linearizing the resulting algebraic equations for Fourier coefficients in the spatial breather tails (where the amplitudes are by assumption small) we arrive at the following linear algebraic equations:

$$k^2 \Omega_b^2 A_{kn} = V''(0) A_{kn} + W''(0) (2A_{kn} - A_{k,n-1} - A_{k,n+1}). \quad (6)$$

If $k\Omega_b = \omega_q$, the solution to (6) is $A_{k,n} = c_1 e^{iqn} + c_2 e^{-iqn}$. Any nonzero (whatever small) amplitude $A_{k,n}$ will thus oscillate without further spatial decay, contradicting the initial assumption. If however

$$k\Omega_b \neq \omega_q \quad (7)$$

for any integer k and any q , then the general solution to (6) is given by $A_{k,n} = c_1 \kappa^n + c_2 \kappa^{-n}$ where κ is a real number depending on ω_q , Ω_b and k . It always admits an (actually exponential) spatial decay by choosing either c_1 or c_2 to be nonzero. In order to fulfill (7) for at least one real value of Ω_b and any integer k , we have to request $|\omega_q|$ to be bounded from above. That is precisely the reason why the spatial lattice is needed. In contrast most spatially continuous field equations will have linear spectra

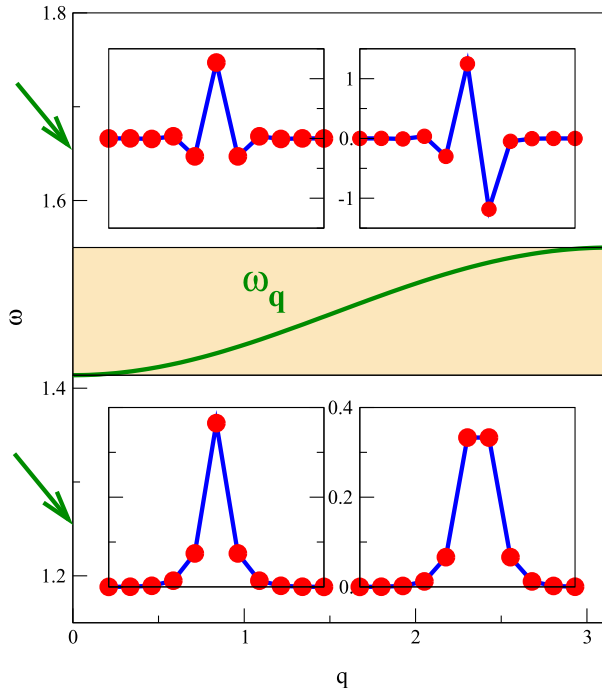


Fig. 1. The frequency versus wavenumber dependence of the linear spectrum for a one-dimensional chain of anharmonic oscillators with potentials (8). Chosen DB frequencies are marked with green arrows and lie outside the linear spectrum ω_q . Red circles indicate the oscillator displacements for a given DB solution, with all velocities equal to zero. Lines connecting circles are guides for the eye. From [9].

which are unbounded. That makes resonances of higher order harmonics of a localized excitation with the linear spectrum unavoidable. The nonresonance condition (7) is thus an (almost) necessary condition for obtaining a time-periodic localized state on a Hamiltonian lattice [8].

The performed analysis can be extended to more general classes of discrete lattices, including e.g. long-range interactions between sites, more degrees of freedom per each site, higher-dimensional lattices etc. But the resulting non-resonance condition (7) keeps its generality, illustrating the key role of discreteness and nonlinearity for the existence of discrete breathers.

Let us show discrete breather solutions for various lattices. We start with a chain (1) with the functions

$$V(x) = x^2 + x^3 + \frac{1}{4}x^4, \quad W(x) = 0.1x^2. \quad (8)$$

The spectrum ω_q is optic-like and shown in Fig. 1. Discrete breather solutions can have frequencies Ω_b which are located both below and above the linear spectrum. The time-reversal symmetry of (2) allows to search for DB displacements $x_n(t=0)$ when all velocities $\dot{x}_n(t=0) = 0$. These initial displacements are computed with high accuracy (see following sections) and plotted in the insets in Fig. 1 [9]. We show solutions to two DB frequencies located above and below ω_q - their actual values are marked with the green arrows. To each DB frequency we show two different spatial DB patterns - among an infinite number of other possibilities, as we will see below. The high-frequency DBs ($\Omega_b \approx 1.66$) occur for large-amplitude, high-energy motion with adjacent particles moving out of phase. Low-frequency DBs ($\Omega_b \approx 1.26$) occur for small-amplitude motion with adjacent particles moving in phase.

In Fig. 2 we show two DB solutions for a Fermi-Pasta-Ulam chain of particles coupled via anharmonic springs $V(x) = 0, W(x) = \frac{1}{2}x^2 + \frac{1}{4}x^4$ (c.f. (1)) which has an acoustic-type spectrum [11]. The DB frequency is in both cases $\Omega_b = 4.5$. Again the displacements x_n are shown for an initial time when all velocities vanish. In the inset we plot the strain $u_n = x_n - x_{n-1}$ on a log-normal scale. The DB solutions are exponentially localized in space.

Finally we show DB solutions for a *two-dimensional* square lattice of anharmonic oscillators with

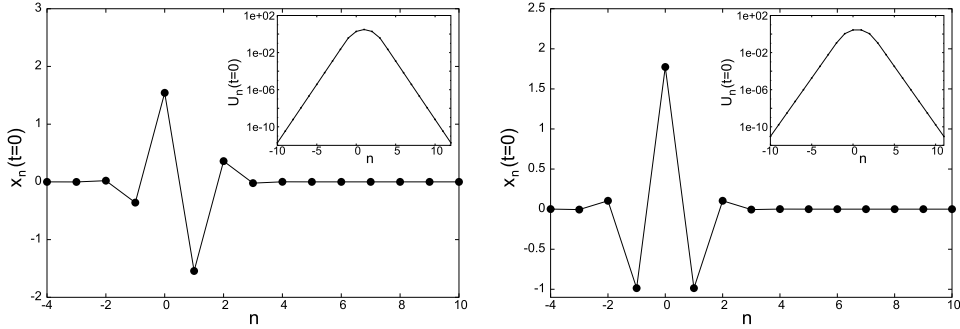


Fig. 2. Discrete breather solutions for a Fermi-Pasta-Ulam chain (see text). These states are frequently referred to as the Page mode (left) and the Sievers-Takeno mode (right). Adapted from [11].

nearest neighbour coupling. The equations of motion read

$$\ddot{x}_{i,j} = k(x_{i+1,j} + x_{i-1,j} - 2x_{i,j}) + k(x_{i,j+1} + x_{i,j-1} - 2x_{i,j}) - x_{i,j} - x_{i,j}^3 \quad (9)$$

with oscillator potentials $V(x) = \frac{1}{2}x^2 + \frac{1}{4}x^4$. In Fig. 3 we plot the oscillator displacements with all velocities equal to zero for three different DB frequencies and $k = 0.05$ [12]. For all cases adjacent oscillators move out of phase.

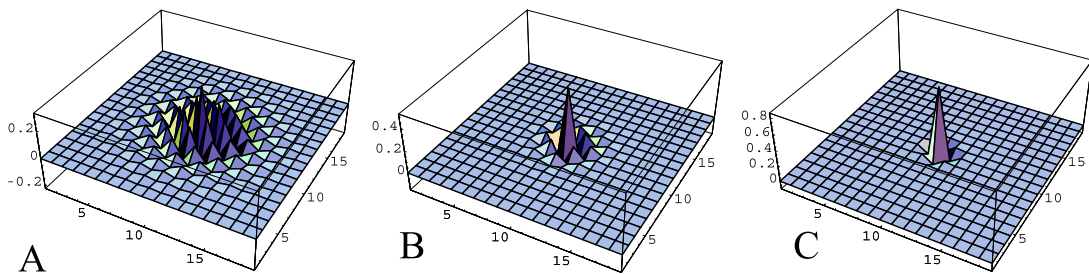


Fig. 3. Displacements of DBs on a two-dimensional lattice (9) with $k = 0.05$, all velocities equal to zero. (A) $\Omega_b = 1.188$; (B) $\Omega_b = 1.207$; (C) $\Omega_b = 1.319$. From [12].

We emphasize that DB solutions can be typically localized on a few lattice sites, regardless of the lattice dimension. Thus little overall coherence is needed to excite a state nearby - just a few sites have to oscillate coherently, the rest of the lattice does not participate strongly in the excitation.

3. Spatial localization

Let us discuss the localization properties of discrete breathers. Consider a model with one degree of freedom per unit cell. Generalizations to more complicated cases should be straightforward. The Hamiltonian reads

$$H = \sum_l \left[\frac{1}{2} P_l^2 + V(X_l) + \sum_{l'} W_{l,l'} (X_l - X_{l'}) \right]. \quad (10)$$

The hypercubic lattice has dimension d , and the lattice index l is a d -dimensional vector with integer components. The interaction potential $W_{l,l'} = W_{l+m,l'+m}$, and thus the model, are translationally invariant. All zero and first derivatives of the potential functions vanish for zero arguments. By the virtue of the discreteness the frequency spectrum ω_q of small amplitude plane waves is bounded in absolute value.

A discrete breather solution is given by

$$X_l(t) = \sum_k A_{kl} e^{ik\Omega_b t}. \quad (11)$$

Here the Fourier number k is a scalar integer independent of the lattice dimension d . The breather is localized in space which implies

$$A_{k,|l|\rightarrow\infty} \rightarrow 0. \quad (12)$$

Assuming that the potential functions have nonzero second derivatives at their origin, i.e. $V''(0) = v_2 \neq 0$ and $W''_{0,l} = w_{0,l} \neq 0$ for some l , we may linearize the algebraic equations for the Fourier coefficients A_{kl} in the spatial tails $|l| \rightarrow \infty$:

$$k^2 \Omega_b^2 A_{kl} = v_2 A_{kl} + \sum_{l'} w_{l,l'} (A_{kl} - A_{kl'}). \quad (13)$$

Since the Fourier amplitude equations decouple after linearization, we can solve each of these equations separately. Recalling that the necessary condition for the localization of each Fourier amplitude is the nonresonance condition $k\Omega_b \neq \omega_q$, the spatial decay of the k -th amplitude is then given by the lattice Green's function

$$G_\lambda(l) = \int_{1.BZ} \frac{\cos(ql)}{\omega_q^2 - \lambda} d^d q, \quad \lambda = k^2 \Omega_b^2. \quad (14)$$

Here the integration extends over the first Brillouin zone of the reciprocal wavevector space q . We note that the spectrum ω_q is periodic in q , with its irreducible multidimensional period residing exactly in the first Brillouin zone. Fixing the direction of l and changing its absolute value, Eq. (14) will then generate the Fourier coefficients of the periodic function $(\omega_q^2 - \lambda)^{-1}$. The spatial decay of the breather is thus characterized by the convergence properties of the corresponding Fourier series. And the convergence properties of Fourier series are defined through the analytical properties of the generating periodic function.

3.1 Optical breathers

3.1.1 Short range interactions

We define a lattice having short-range interactions, if the corresponding squared spectrum ω_q^2 is an analytical function on the extended wavevector space q , e.g. when all its derivatives at any point q exist and are finite. Examples are lattices with nearest neighbour interaction, or more general lattices with finite-size interactions where $w_{0,l} = 0$ for $|l| > r$ with r being a positive real number. But we can even generalize by considering lattices where the harmonic interaction potential extends over the whole lattice, with exponentially decaying amplitudes $w_{0,l} \sim e^{-|l|/r}$ for $|l| \gg r$. For all these cases the denominator $(\omega_q^2 - \lambda)^{-1}$ which enters (14) is an analytical periodic function of q , and thus the convergence of its Fourier series and the spatial localization of a DB is bounded by exponential tails. The exponent will depend on $\lambda = k^2 \Omega_b^2$. The localization length will grow whenever any of the multiples $k\Omega_b$ will come close to an edge of the spectrum ω_q .

In the insets in Fig. 2 the exponential localization of two DBs is shown for a one-dimensional FPU chain with nearest neighbour interaction. The comparison between the numerically obtained localization length and the prediction from Eq. (14) is reviewed extensively in [8].

Here we also show the amplitude distribution of a DB solution for a three-dimensional cubic DNLS lattice with nearest neighbour interaction

$$\dot{\Psi}_l = i(\Psi_l + |\Psi_l|^2 \Psi_l + 0.1 \sum_{m \in N_l} \Psi_m), \quad (15)$$

where N_l denotes the set of nearest neighbours of l . Making the substitution $\Psi_l = A_l e^{i\Omega_b t}$ the algebraic equations are solved for the real amplitudes A_l [13] for a lattice with linear size 31. To visualize the solution, we place the DB center at the lattice site $l = (16, 16, 16)$ and plot its amplitude distribution as a function of the x, y coordinates in a plane with fixed coordinate $z = 16$ which contains the lattice site with the maximum breather amplitude. Note that the DB is strongly localized on a few lattice sites (left plot in Fig. 4). The same solution, when displayed on a logarithmic amplitude scale, shows a conical structure (right plot in Fig. 4) as expected from the predicted exponential decay in space.

3.1.2 Long range interactions

We define a lattice having long-range interactions, if the corresponding squared spectrum ω_q^2 is a nonanalytical function on the extended wavevector space q , i.e. some of its derivatives at some points

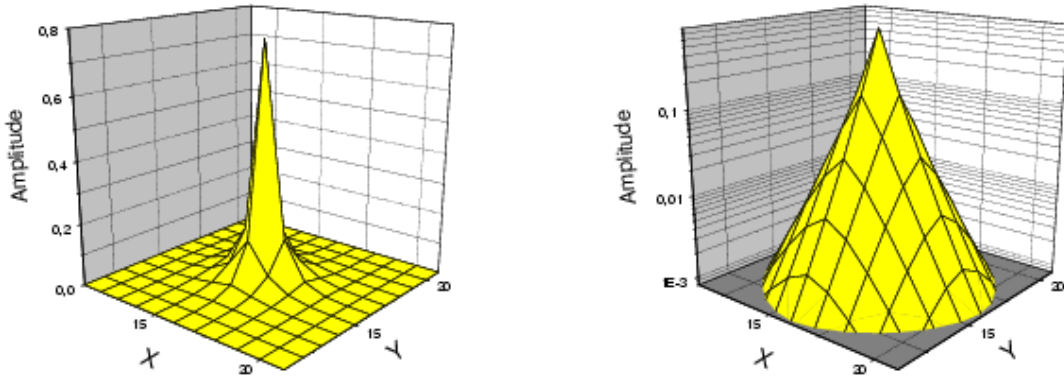


Fig. 4. Amplitude distribution of a breather solution of the the three-dimensional DNLS system (15) with linear size $N = 31$. Only a distribution in a cutting $(x; y)$ plane is shown (the plane cuts the center of the breather). The intersections of the grid lines correspond to the actual amplitudes, the rest of the grid lines are guides to the eye. Left panel - amplitudes are shown on a linear scale. Right panel - the same solution with amplitudes plotted on a logarithmic scale. Data are from Fig. 2 in [13].

q do not exist or diverge. That happens e.g. when the harmonic interaction potential extends over the whole lattice, and decays algebraically with increasing distance $w_{0,l} \sim |l|^{-s}$ with some positive exponent s . Despite the slow decay of interactions, discrete breathers still exist, but will now localize slower than exponentially. In fact what matters is the analysis of the degree of nonanalyticity of ω_q^2 , which straightforwardly gives a power law convergence of the Fourier series (14) and thus an algebraic spatial localization of DBs.

We will present the results obtained in [14] to illustrate that the true DB localization can be more complicated even for simple one-dimensional lattices. We consider the Hamiltonian

$$H = \sum_l \left[\frac{1}{2} P_l^2 + V(X_l) + \sum_{l'} W_{|l-l'|} (X_l - X_{l'}) \right]. \quad (16)$$

The on-site potential $V(z) = \sum_{\mu=2}^{\infty} \frac{v_{\mu}}{\mu} z^{\mu}$ generates an optical phonon spectrum, and the interaction $W_l(z) = \sum_{\mu=2}^{\infty} \frac{\phi_{\mu}(l)}{\mu} z^{\mu}$ incorporates long range interactions with $\phi_2(l) = \frac{C}{2} \frac{1}{l^s}$. For small values of P_l and X_l the classical Hamiltonian equations of motion $\dot{X}_l = \frac{\partial H}{\partial P_l}$, $\dot{P}_l = -\frac{\partial H}{\partial X_l}$ can be linearized in X_l . Solving the corresponding eigenvalue problem with plane waves $X_l(t) \sim \exp^{i(ql - \omega_q t)}$, one obtains

$$\omega_q^2 = v_2 + 2C \sum_{m=1}^{\infty} \frac{1}{m^s} (1 - \cos(qm)). \quad (17)$$

Let us discuss the properties of $E_s(q) = \omega_q^2 \geq 0$. $E_s(q)$ is bounded from above for all $s > 1$ and periodic in q with period 2π . Most important is that $E_s(q)$ is a nonanalytic function in q , i.e. its $\kappa = (s - 1)$ -st derivative with respect to q is discontinuous at $q = 0$ (when s is noninteger, $(s - 1) < \kappa < s$). This follows already from the fact that the convergence radius of (17) is zero for nonzero imaginary components in q . Indeed for even integers s one finds $(E_s(q) - v_2) \sim B_s(q/(2\pi))$ for $0 \leq q \leq 2\pi$. Here $B_s(z)$ is the Bernoulli polynomial of s -th order. Consequently at small q the expansion of $E_s(q)$ contains a term q^{s-1} which, together with the periodicity of $E_s(q)$, leads to the mentioned nonanalyticity. For odd integers s the expansion of $E_s(q)$ contains a term $q^{s-1} \ln(q)$, and for noninteger s a term q^{s-1} (follows from $d^2 E_s(q)/dq^2 = -E_{s-2}(q) + 2C\zeta(s-2)$ with $\zeta(z)$ being the Riemann Zeta function). Finally for small q the leading term in the expansion of $E_s(q)$ is $v_2 + C\zeta(s-2)q^2$ for $s > 3$ and $v_2 + 2Ca(s)q^{s-1}$ for $1 < s < 3$ with $a(s) = \int_0^{\infty} (1 - \cos x)/x^s dx$. Note that the dispersion at the upper band edge ($q = \pi$) is in leading order always proportional to $(q - \pi)^2$.

Now we can turn to the first problem of the spatial decay of a breather. In order to generate a breather solution we chose $v_4 \neq 0$ and all other anharmonic terms in $V(z)$ and $W(z)$ being zero. Since we can only simulate finite system sizes N , we use periodic boundary conditions. In that case

we have to define a cutoff length in the interaction which we chose to be $N/2$. Calculated breather solutions for $s = 10, 20, 30$ are shown in Fig. 5. We observe that the spatial decay of the breather is

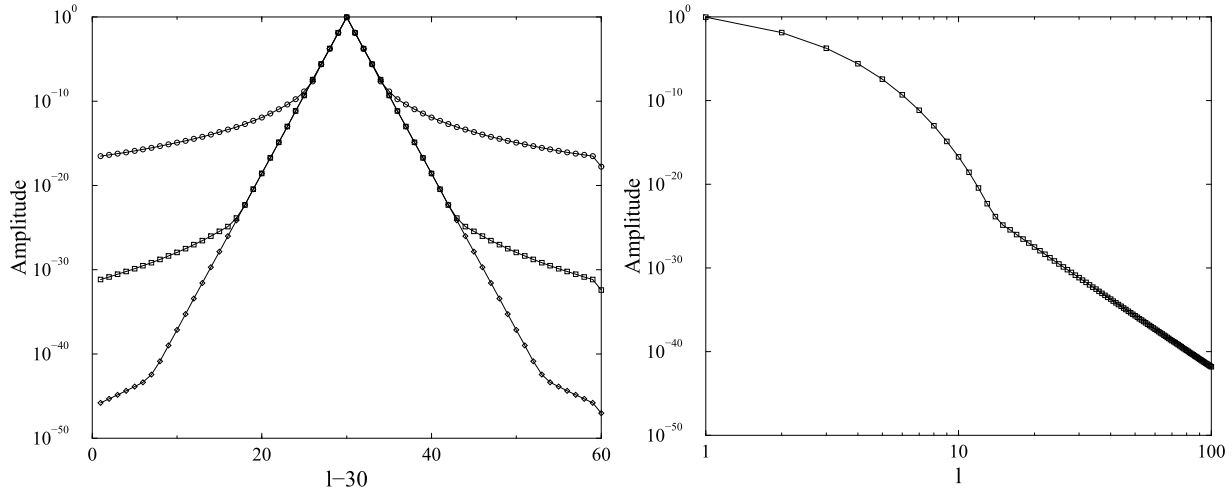


Fig. 5. Left panel: breather solution at time $t = 0$ with $P_l(t = 0) = 0$. The corresponding displacements (amplitudes) $X_l(t = 0)$ are plotted versus lattice site. The nonzero model parameters are $v_2 = v_4 = 1$, $C = 0.01$. The period of the solutions $T = 4.7682$. Circles: $s = 10$, squares: $s = 20$, diamonds: $s = 30$. Lines are guides to the eye. Right panel: same as in left panel but only for $s = 20$ in a log-log plot. Data from [14].

exponential for small distances from the center, while it becomes *algebraic* (in fact exactly $1/l^s$) after a crossover at some distance l_c (see right panel in Fig. 5). Note that l_c is s -dependent. Moreover, l_c is also depending on the parameter which selects a given breather solution from its one-parameter family (this parameter could be the breather frequency, its energy, action or something else).

The asymptotic spatial decay of the breather is given by the convergence properties of the Fourier series (14). Nonanalytic functions with discontinuities in the $(s - 1)$ -st derivative produce Fourier series which converge algebraically $1/l^s$. From that follows that at large distances the spatial decay of the breather will be algebraic, which is what we found in Fig. 5. To obtain the exponential decay at small distances, let us first slide along the breather family such that the breather frequency (or one of its multiples) approaches the edge of the phonon band ω_q . Then the integrand in (14) will become very large for wave numbers close to the band edge which is approached. Applying a stationary phase approximation to (14), i.e. expanding the integrand around the band edge we obtain

$$G_\lambda(l) \sim \int_{-\infty}^{\infty} \frac{\cos(ql)}{v_2 - \lambda + C\zeta(s-2)q^2} dq \quad (18)$$

for $s > 3$ and

$$G_\lambda(l) \sim \int_0^{\infty} \frac{\cos(ql)}{v_2 - \lambda + 2Ca(s)q^{s-1}} dq \quad (19)$$

for $1 < s < 3$. Standard evaluation of (18) (closing the integration contour in the complex plane by adding a half circle with infinite radius and evaluating the residua) yields $G_\lambda(l) \sim e^{-\sqrt{v_2-\lambda}l}$ for $s > 3$, i.e. exponential decay. On the other side, (19) yields (closing the integration contour in the complex plane by adding a quarter circle and returning to zero along the positive imaginary axis, and noticing that there are no poles of the integrand in the enclosed first quadrant including the imaginary axis) $G_\lambda(l) \sim 1/l^s$ for $1 < s < 3$.

Now we can explain the observed crossover from exponential to algebraic decay in Fig. 5. Indeed, the stationary phase approximation for these cases leads to (18) in the limit $(v_2 - \lambda) \rightarrow 0$. This approximation neglects higher order terms in the expansion of $E_s(q)$ around $q = 0$ which necessarily contain nonanalytic terms. Consequently (18) probes (14) for not too large distances. Thus we can explain the observed crossover. We can also estimate the crossover distance l_c using a simple argument. A tagged site with index $l < l_c$ and $l > 0$ (the center of the breather is located at $l_b = 0$)

will experience forces from all other sites with index l' according to (16). The amplitude of these forces will monotonously decay to zero for increasing l' with $l' > l$. However the amplitude of the forces for decreasing l' will be given by $(l-l')^{-s}e^{\nu(l-l')}$ for $0 < l' < l$ (here ν is the given exponent of the spatial decay for $|l| < l_c$). Since for negative l' the amplitude of these forces will again monotonously decay to zero, the worst case is reached when $l' = 0$. If this force acting from the center of the breather on site l is comparable to the forces acting on l from its nearest neighbours, the exponential decay will be violated. This condition yields $l_c^{-s}e^{\nu l_c} = 1$ or

$$\frac{\ln l_c}{l_c} = \frac{\nu}{s}. \quad (20)$$

Especially we find that $l_c \rightarrow \infty$ if $\nu/s \rightarrow 0$. Thus for $s > 3$ exponential decay is reobtained either for large s or for breathers with frequencies close to the phonon band edge. Since we are considering a lattice, the exponential decay part will disappear if $l_c \approx 1$ or smaller. For $s = 20$ and $\nu = 4.2724$ we obtain $l_c = 11.39$, and for $s = 30$ and the same value of ν the result is $l_c = 21.56$. We miss the observed crossovers in Fig. 5 by just two sites.

3.2 Acoustic breathers

As already mentioned, the breather frequency Ω_b should fulfill a nonresonance condition $n\Omega_b \neq \omega_q$ for all integer $n = 0, \pm 1, \pm 2, \dots$. This is necessary in general in order to have spatial localization of the corresponding Fourier mode. In the case of weakly coupled oscillators a proper choice of the breather frequency always ensures nonresonance. In the case of homogeneous interaction potentials the symmetry of the potential $\Phi(z) = \Phi(-z)$ is found also in the breather solution, which implies that only odd Fourier components are present in the breather solution. Thus the dc component ($0 \times \Omega_b = 0$) which is in resonance with the mentioned degenerated phonon band is strictly zero, and the resonance is harmless.

If any nonzero multiple of Ω_b resonates even with an edge of a phonon band, this leads either to the vanishing of the whole breather, or to a delocalization of the breather and to a divergence of its energy. The resonance of the dc component to be considered here is special - it resonates with a Goldstone mode, and one can expect the resonance to be not as destructive to the breather as any resonance at nonzero frequency. From the theory of elastic defects we know the characteristic feature of the strain decay to be algebraic in the distance (from the defect center). The exponent is only depending on the dimension of the system and on the symmetry of the defect (monopole, dipole etc.), but independent on the defect strength.

We will treat the simplest case of hypercubic lattices with one degree of freedom per lattice site and nearest neighbour interaction, which can be considered as generalized Fermi-Pasta-Ulam (FPU) systems:

$$H = \sum_l \left[\frac{1}{2} P_l^2 + \sum_{l' \in \text{DNN}} \Phi(X_l - X_{l'}) \right]. \quad (21)$$

Here P_l and X_l are canonically conjugated scalar momenta and displacements of a particle at lattice site l . Note that depending on the lattice dimension d the lattice site label l is a d -component vector with integer components. The inner sum in (21) goes over all *directed nearest neighbours*, e.g. for $d = 1$ and $l = n$ we sum over $l' = n+1$, for $d = 2$ and $l = (n, m)$ we sum over $l' = \{(n+1, m); (n, m+1)\}$ etc. The interaction potential $\Phi(z)$ is given by

$$\Phi(z) = \frac{1}{2}\phi_2 z^2 + \frac{1}{3}\phi_3 z^3 + \frac{1}{4}z^4, \quad (22)$$

which turns out to be generic enough for the purposes discussed below.

Breathers for such a system can be represented in the form (11). We will restrict ourselves to solutions invariant under time reversal, so that all $A_{kl} = A_{-k,l}$ are real. The spatial localization property of (11) implies $A_{k,|l| \rightarrow \infty} \rightarrow 0$ for $k \neq 0$ and $A_{0,|l| \rightarrow \infty} \rightarrow \text{const.}$ The dc component of the breather is given by A_{0l} .

Numerical and approximative analytical studies for one-dimensional lattices show that the acoustic breather exists as a solution to finite energy. Its peculiarity is that the dc component of the breather versus lattice site number has a kink shape $A_{0,l \rightarrow \pm\infty} \rightarrow \pm\text{const.}$ for free boundaries (Fig. 6). For

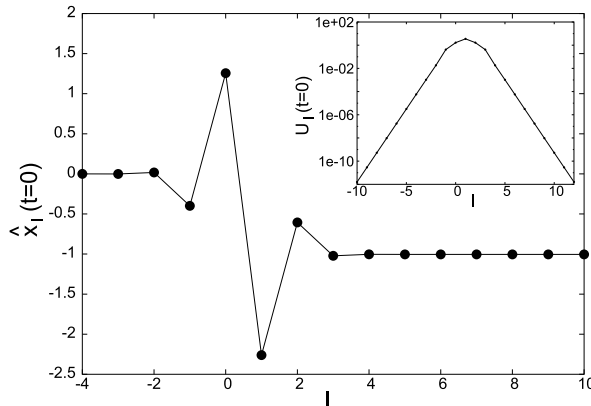


Fig. 6. An acoustic DB solution for the $d = 1$ case. Displacements $X_l(t = 0)$ for $\phi_2 = \phi_3 = \phi_4 = 1$ and $\Omega_b = 4.5$ are plotted versus lattice site number l . At this initial time all velocities $P_l(t = 0) = 0$. Inset: Staggered deformation $u_l = (-1)^l(x_l - x_{l-1})$ for the same solution on a logarithmic scale versus lattice site number l . This DB is linearly unstable. Data from [11].

periodic boundary conditions one would find a linear decay of A_{0l} far from the breather, but the gradient of the dc components (the strain) is inverse proportional to the size of the chain, so that in the limit of an infinite chain the result is again a constant for the dc component (zero strain).

Let us now turn to the general d -dimensional case. Suppose that a breather exists, which creates some strain field. The dc displacements A_{0l} will have some dependence on the lattice site vector l . The strain E_l is given by the lattice gradient of A_{0l} . The far field energy is given by the integral over the squared strain. Assuming that the strain does decay algebraically, we can use continuum theory far from the breather. The corresponding equation is equivalent to the electrostatic equations in d dimensions. Consider $d = 1$. A monopole far field $E = c \neq 0$ and the corresponding energy diverges. Also in this case the (electrostatic) potential $A_{0l} = \text{sgn}(l)a + cl$. This is clearly not what was observed for acoustic breathers in 1d. A dipole far field instead will yield $E = 0$, $A_{0l} = \text{sgn}(l)a$, and the energy is finite. This is the situation observed. So the known acoustic breather solutions are accompanied by a dipole strain field. The request that the acoustic breather is a solution to finite energy limits the strain fields to dipole or higher order multipole symmetries. In this special case the potential A_{0l} is constant far away from the breather, so the corresponding exponent of the algebraic decay is simply zero.

For $d = 2$ (square lattice) the situation is the following. A monopole will generate a strain $E \sim 1/l$ and a potential $A_{0l} \sim \ln(l)$. The energy of such a field diverges. If we search for acoustic breathers with finite energy, we would have to exclude a monopole field. A dipole generates a strain $E \sim 1/l^2$ (we skip angular dependencies here) and a potential $A_{0l} \sim 1/l$. The energy for this field is finite. The predicted exponents of the algebraic decay are nonzero, and no simple limit exists, which makes the strain to be of compact support. So already at this stage it is clear, that existence proofs of acoustic breathers in two-dimensional systems are much more complicated than for $d = 1$. Notice that for $d = 3$ (cubic lattice) a monopole generates $E \sim 1/l^2$ and the energy of this field is finite.

Next we will present numerical calculations of acoustic breathers of (21) for $d = 2$ and $\phi_2 = \phi_3 = 0.01$ [15]. The results show up to numerical accuracy that acoustic breathers exist on finite lattices with free boundaries. The symmetry and spatial decay properties are in accord with the expectations given above. The maximum lattice size is 70×70 , but no profound size effects were observed on the existence and symmetry of the acoustic breather when considering smaller systems. The only size effect (to be expected) is observed even for the largest systems with respect to the algebraic decay properties. The ac components of the found solution decay exponentially in space and essentially

vanish at a distance of 5-7 lattice constants from the center of the breather. In Fig. 7 we show the dc

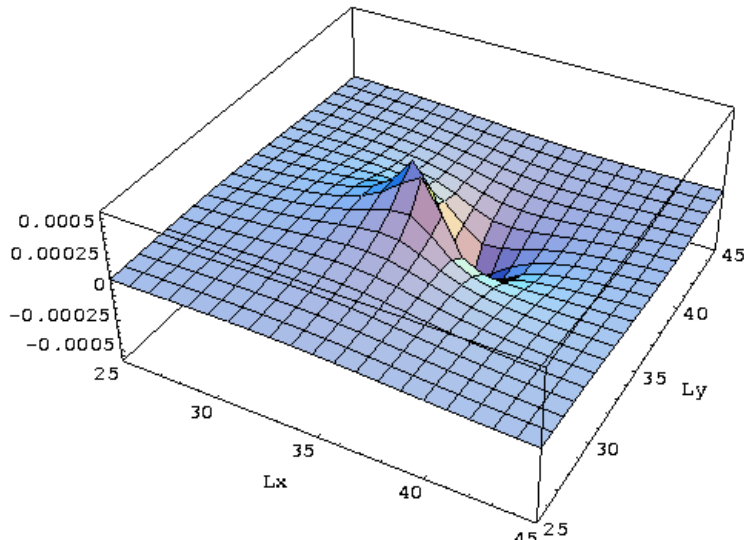


Fig. 7. Dc displacements of a breather as a function of the lattice vector l . Figure from [15].

displacements of a DB solution. We do observe dipole symmetry of the dc field.

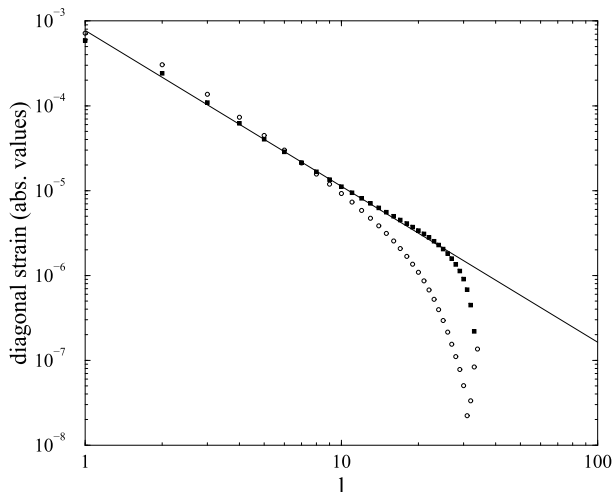


Fig. 8. Variation of the absolute value of the strain along the diagonals of the lattice on a double logarithmic plot. Open circles - (1,1) direction; filled squares - (-1,1) direction. Figure from [15].

To analyse the spatial behaviour of the strain, we plot in Fig. 8 the variation of the absolute values of the strain along the two diagonals, as in those directions we have the largest distance and can hope that finite size effects are suppressed in some bulk region. The results depend on the choice of the diagonal. The diagonal which is directed along the dipole moment gives poor results - the finite size effects are too strong to observe any power law in the double logarithmic plot. The second diagonal perpendicular to the dipole moment however, though still with strong influence from the boundaries, allows to fit some part of the bulk data with a power law (solid line in Fig. 8). The resulting exponent is 1.85, and considering the small system size, quite close to the expected value 2.

These results support the expectations that breathers can exist in real crystals. Moreover at any finite temperature excited breathers will decay after some time. Since they are accompanied by a strain field, those strain fields will be dispersed in the form of low-lying acoustic modes after the decay of a breather. Thus breathers can act as an efficient energy transfer from high-frequency excitations into low-frequency acoustic phonons.

3.3 Nonlinear corrections

The linearization of the equations of motion in the spatial tail of a DB seems to be fine by virtue of the localized character of the solution. Yet there may be nonlinear corrections in the tails, which will happen typically whenever any of the multiples of the DB frequency comes close to the spectrum ω_q . While the Fourier amplitude A_{kl} with the weakest spatial decay, as predicted from linearization, will always decay accordingly, it will do so very slowly by the above assumption. Consequently nonlinear terms which contain this amplitude and enter the equations for other Fourier amplitudes, e.g. the one with $k' = 3k$, will induce a nonlinear but much slower spatial decay than the linearized one. A detailed discussion is given in [8]. Here we want to add that these nonlinear corrections also allow to systematically account for the surprising localization of all higher harmonics of a breather solution in the continuous sine-Gordon equation, despite the fact that ω_q is unbounded there. It comes together with the property of the sine-Gordon equation being integrable. This implication of a (perhaps uncountable) infinite number of conservation laws is equivalent to a corresponding number of symmetries confining the dynamics to high dimensional tori no matter where one starts in phase space. It has been since conjectured that it is these symmetries which for some reason also guarantee that the breather exists, since one has to satisfy an infinite number of additional constraints - one for each resonant higher harmonics - in order to suppress the nondecaying linear solution for it, leaving one with the nonlinear correction only.

4. Energy thresholds of discrete breathers

DB solutions come in one-parameter families. The parameter can be the amplitude (measured at the site with maximum amplitude), the energy E or the breather frequency Ω_b . Its amplitude can be lowered to arbitrarily small values, at least for some of the families for an infinite lattice. In this zero amplitude limit, the DB frequency Ω_b approaches an edge of the phonon spectrum ω_q . This happens because the nonresonance condition $\omega_q/\Omega_b \neq 0, 1, 2, 3, \dots$ has to hold for all solutions of a generic DB family. In the limit of zero amplitude, the solutions have to approach solutions of the linearized equations of motion, thus the frequency Ω_b has to approach some ω_q , but at the same time not to coincide with any phonon frequency. This is possible only if the breather's frequency tends to an edge ω_E of the phonon spectrum in the limit of zero breather amplitude. If we consider the family of nonlinear plane waves which yields the corresponding band edge plane wave in the limit of zero amplitude A , then its frequency ω will depend on A like

$$|\omega - \omega_E| \sim A^z \quad (23)$$

for small A , where the detuning exponent z depends on the type of nonlinearity of the Hamiltonian (10).

Here we follow the lines of argumentation in [13]. Let us assume that we have a system with short range interactions and estimate the discrete breather energy in the limit of small amplitudes. Define the amplitude of a DB to be the largest of the amplitudes of the oscillations over the lattice. Denote it by A_0 where we define the site $l = 0$ to be the one with the largest amplitude. The amplitudes decay in space away from the breather center, and by linearising about the equilibrium state and making a continuum approximation, the decay is found to be given by $A_l \sim CF_d(|l|\delta)$ for $|l|$ large, where F_d is a dimension-dependent function

$$F_1(x) = e^{-x} \quad , \quad F_3(x) = \frac{1}{x} e^{-x} \quad (24)$$

$$F_2(x) = \int \frac{e^{-x\sqrt{1+\zeta^2}}}{\sqrt{1+\zeta^2}} d\zeta, \quad (25)$$

δ is a spatial decay exponent to be discussed shortly, and C is a constant which we shall assume can be taken of order A_0 . To estimate the dependence of the spatial decay exponent δ on the frequency of the time-periodic motion Ω_b (which is close to the edge of the linear spectrum) it is enough to consider the dependence of the frequency of the phonon spectrum ω_q on the wave vector q when

close to the edge. Generically this dependence is quadratic $(\omega_E - \omega_q) \sim |q - q_E|^2$ where $\omega_E \neq 0$ marks the frequency of the edge of the linear spectrum and q_E is the corresponding edge wave vector. Then analytical continuation of $(q - q_E)$ to $i(q - q_E)$ yields a quadratic dependence $|\Omega_b - \omega_E| \sim \delta^2$. Finally we must insert the way that the detuning of the breather frequency from the edge of the linear spectrum $|\Omega_b - \omega_E|$ depends on the small breather amplitude. Assuming that the weakly localized breather frequency detunes with amplitude as the weakly nonlinear band edge plane wave frequency this is $|\Omega_b - \omega_E| \sim A_0^z$. Then $\delta \sim A_0^{z/2}$.

Now we are able to calculate the scaling of the energy of the discrete breather as its amplitude goes to zero by replacing the sum over the lattice sites by an integral

$$E_b \sim \frac{1}{2} C^2 \int r^{d-1} F_d^2(\delta r) dr \sim A_0^{(4-zd)/2}. \quad (26)$$

This is possible if the breather persists for small amplitudes and is slowly varying in space. We find that if $d > d_c = 4/z$ the breather energy diverges for small amplitudes, whereas for $d < d_c$ the DB energy tends to zero with the amplitude. Inserting $z = 2$ we obtain $d_c = 2$. Note that for $d = d_c$ logarithmic corrections may apply to (26), which can lead to additional variations of the energy for small amplitudes.

An immediate consequence is that if $d \geq d_c$, the energy of a breather is bounded away from zero. This is because for any non-zero amplitude the breather energy can not be zero, and as the amplitude goes to zero the energy goes to a positive limit ($d = d_c$) or diverges ($d > d_c$). Thus we obtain an energy threshold for the creation of DBs for $d \geq d_c$. This new energy scale is set by combinations of the expansion coefficients in (10). If $z = 2$ with $|\Omega - \omega_E| \sim \beta A^2$ for the nonlinear plane waves, and the energy per oscillator $E \sim gA^2$ and the spatial decay exponent δ is related by $|\Omega_b - \omega_E| \sim \kappa \delta^2$, then the energy threshold E_{min} is of the order of $\kappa g / \beta$, and the minimum energy breather in 3D has spatial size of the order of the lattice spacing, independently of κ, g and β . One should allow for a factor of $(2 + d)$ for underestimating the true height of the minimum and the contributions of nearest neighbours.

Many numerical results have since confirmed the above results. For the d-dimensional DNLS model (15) the left panel in Fig. 9 shows the variation of the DB energy with its central amplitude, and a clear notion of an energy threshold starting with $d = 2$ [13]. The minimum energy DB profile for $d = 3$ is the one plotted in Fig. 4 and is indeed (still) strongly localized on the lattice. In order to observe the effect energy thresholds in one dimension, we present results for a modified DNLS system in one spatial dimension $d = 1$:

$$\dot{\Psi}_l = i(\Psi_l + |\Psi_l|^{\mu-1} \Psi_l + C \sum_{m \in N_l} \Psi_m). \quad (27)$$

By tuning μ we can tune the system into a case with a nonzero energy threshold. In the right panel in Fig. 9 we show results for $d = 1$ and $\mu = 3, 5, 7$. Again we find full agreement with the predictions from above. Note that even one-dimensional lattices exhibit positive lower bounds on breather energies if $\mu \geq 5$.

We can predict that a modified DNLS system with an additional term $v_{\mu'} |\Psi_l|^{\mu'-1} \Psi_l$ can exhibit complex curves $E_b(A_0)$. For example, for $d = 1$, $\mu = 7$, $\mu' = 3$ and $v_{\mu'} = 0.1$, the $E_b(A_0)$ -dependence will be nearly identical to the case $v_{\mu'} = 0$ already considered, if the amplitude A_0 is not too small. Then $E_b(A_0)$ will show a minimum at a non-zero value of A_0 . For small A_0 however the energy of the breather will ultimately decay to zero, so the curve has a maximum for smaller amplitudes! The dashed line in the right panel in Fig. 9 shows the numerical calculation, which coincides with our prediction.

Another example is the two-dimensional lattice system (9) which is characterized by $z = 2$, and thus the critical dimension is $d = 2$. The energy thresholds have been computed and reported in [12]. The profiles of DB solutions in Fig. 3 correspond to (A) a low amplitude DB, (B) the minimum energy DB, and (C) a high amplitude DB.

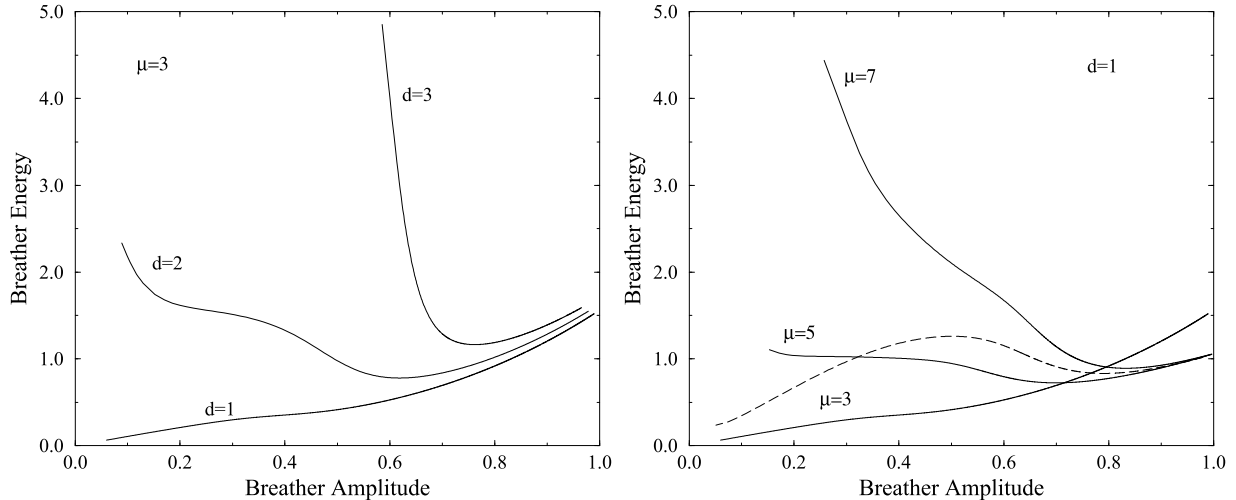


Fig. 9. Left panel: Breather energy versus amplitude for the DNLS system in one, two and three lattice dimensions. System sizes for $d = 1, 2, 3$: $N=100$, $N=25^2$, $N=31^3$, respectively. Right panel: Breather energy versus maximum amplitude for the DNLS system in one lattice dimension and for three different exponents $\mu = 3, 5, 7$ (solid lines). The system size is $N = 100$ and the parameter $C = 0.1$. The dashed line is for the modified system (cf. text). Data are from Figs. 1 and 3 in [13].

5. Fano resonances with discrete breathers

Wave scattering by discrete breathers can yield total reflection of plane waves for wave numbers with nonzero group velocities. The effect is due to the time-periodicity of the DB which induces an effective time-periodic scattering potential for plane waves. It can be interpreted as a destructive interference between different co-existing propagation channels (a detailed discussion of the theory and experimental data including related fields in transport through nanostructures can be found in [16]). The observed total reflection was shown to be closely related to the well-known Fano resonance [17].

To explore the origin of this resonance we consider the simple example of plane wave scattering by a single site DB in the DNLS model (27) with $\mu = 3$. The linear wave spectrum in this model is given by

$$\omega_q = 2C \cos(q), \quad (28)$$

and constitutes the *open channel* of the scattering problem.

Consider a highly localized DB with $\Omega_b \gg C$. The corresponding DB solution $\psi_n = A_n \exp(i\Omega_b t)$ can be approximated by a single site excitation: $A_0^2 = \Omega_b$, $A_{n \neq 0} = 0$. Due to the gauge invariance of the DNLS model, there are only two propagation channels for an incident small amplitude plane wave [17]. With $X_n \equiv e_{n,0}$ and $Y_n \equiv e_{n,-2}$, the coupled equations for the two channels are [17]:

$$\omega_q X_n = C(X_{n+1} + X_{n-1}) + \Omega_b \delta_{n,0} (2X_0 + Y_0), \quad (29)$$

$$(2\Omega_b - \omega_q) Y_n = C(Y_{n+1} + Y_{n-1}) + \Omega_b \delta_{n,0} (2Y_0 + X_0). \quad (30)$$

It is straightforward to show, that $2\Omega_b - \omega_q \neq \omega_{q'} \forall q, q'$, so that the channel Y_n is always *closed*.

It is instructive to consider a generalised problem given by [17]

$$\omega_q X_n = C(X_{n+1} + X_{n-1}) - \delta_{n,0} (V_x X_0 + V_a Y_0), \quad (31)$$

$$(\Omega - \omega_q) Y_n = C(Y_{n+1} + Y_{n-1}) - \delta_{n,0} (V_y Y_0 + V_a X_0), \quad (32)$$

which is reduced to the system (29,30) when $\Omega = 2\Omega_b$, $V_x = V_y = 2V_a = -2\Omega_b$. Note, that for a particular case $V_a = 0$, i.e. when the closed channel Y is completely uncoupled from the open channel X , the former possesses exactly one localized eigenstate for nonzero V_y [17]:

$$\omega_L^{(y)} = \Omega - \sqrt{V_y^2 + 4C^2}. \quad (33)$$

Using the transfer matrix technique, the transmission coefficient T for the generalized problem (31,32) is given by [17]:

$$T = \frac{4 \sin^2 q}{\left(2 \cos q - a - \frac{d^2 \kappa}{2 - b\kappa}\right) + 4 \sin^2 q} \quad (34)$$

$$a = \frac{V_x + \omega_q}{C}, \quad b = \frac{V_y + \Omega - \omega_q}{C}, \quad d = \frac{V_a}{C}, \quad (35)$$

where κ is the inverse localization length of the closed channel:

$$\kappa = \frac{\Omega - \omega_q + \sqrt{(\Omega - \omega_q)^2 - 4C^2}}{2C}. \quad (36)$$

The transmission coefficient T vanishes, when the condition

$$2 - b\kappa = 0 \quad (37)$$

is satisfied. It is equivalent to the resonance condition $\omega_q = \omega_L^{(y)}$, which has a clear physical meaning: total reflection occurs when the frequency of the incoming wave ω_q in the open channel X resonates with that of the local mode $\omega_L^{(y)}$ of the closed channel Y . Thus the resonance is equivalent to the Fano resonance [18], resulting from a local state interacting and resonating with the continuum of extended states. An intriguing peculiarity of the case under consideration is that the local state itself (belonging to the closed channel) is created *dynamically*, through an *interaction* between the incoming plane wave and the scattering DB.

Coming back to the original problem (29,30), the transmission coefficient is given by

$$T = \frac{4 \sin^2 q}{\left(\frac{2\Omega_b}{C} - \frac{\Omega_b^2}{2C^2} \frac{\kappa}{1 + \kappa \cos q}\right)^2 + 4 \sin^2 q}. \quad (38)$$

For highly localized DBs with $\Omega_b/C \gg 1$ the total reflection occurs in a close vicinity of $q = \pi/2$.

6. Outlook

Armed with the fundamental understanding of the origin of DBs/ILMs through the combination of discreteness with nonlinearity, experimentalists are becoming increasingly proficient at discovering—or creating—new physical systems in which to study DBs/ILMs and their properties. In sum, the theoretical, numerical, and experimental results, as well as the innovative concepts, associated with the physics of DBs/ILMs have shed considerable light on the complex dynamics, properties, and functions of nonlinear discrete physical systems from the nanoscale to the macroscale. The study of such systems and DBs/ILMs they support underpins applications ranging from smart materials that respond collectively to external stimuli in a coherent, tunable fashion to light-induced, reconfigurable all-optical networks. Only a decade ago, DBs/ILMs were almost exclusively the province of theorists. Today, the rapidly expanding list of experimental observations not only establishes the ubiquity of discrete breathers and intrinsic localized modes in nonlinear, discrete physical systems but also generates exciting possibilities for future applications both in fundamental science and in technology. Clearly, for DBs/ILMs, the best is yet to be.

References

- [1] P.W. Anderson, “Absence of diffusion in certain random lattices,” *Phys. Rev.*, vol. 109, p. 1492, 1958.
- [2] A.A. Ovchinnikov, “Localized long-lived vibrational states in molecular crystals,” *Soviet Physics JETP*, vol. 30, p. 147, 1970.
- [3] A.J. Sievers and S. Takeno, “Intrinsic localized modes in anharmonic crystals,” *Phys. Rev. Lett.*, vol. 61, p. 970, 1988.

- [4] S. Flach and C.R. Willis, “Localized excitations in a discrete Klein-Gordon system,” *Phys. Lett. A*, vol. 181, p. 232, 1993.
- [5] S. Flach, “Conditions on the existence of localized excitations in nonlinear discrete systems,” *Phys. Rev. E*, vol. 50, p. 3134, 1994.
- [6] R.S. MacKay and S. Aubry, “Proof of existence of breathers for time-reversible or Hamiltonian networks of weakly coupled oscillators,” *Nonlinearity*, vol. 7, p. 1623, 1994.
- [7] S. Aubry, “Breathers in nonlinear lattices: Existence, linear stability and quantization,” *Physica D*, vol. 103, p. 201, 1997.
- [8] S. Flach and C.R. Willis, “Discrete breathers,” *Phys. Rep.*, vol. 295, p. 181, 1998.
- [9] D.K. Campbell, S. Flach, and Y.S. Kivshar, “Localizing energy through nonlinearity and discreteness,” *Physics Today*, vol. 57, no. 1, pp. 43–49, 2004.
- [10] S. Flach and A.V. Gorbach, “Discrete breathers – Advances in theory and applications,” *Phys. Rep.*, vol. 467, p. 1, 2008.
- [11] S. Flach and A.V. Gorbach, “Discrete breathers in Fermi-Pasta-Ulam lattices,” *Chaos*, vol. 15, p. 015112, 2005.
- [12] M. Eleftheriou and S. Flach, “Discrete breathers in thermal equilibrium: distributions and energy gaps,” *Physica D*, vol. 202, p. 142, 2005.
- [13] S. Flach, K. Kladko, and R.S. MacKay, “Energy thresholds for discrete breathers in one-, two-, and three-dimensional lattices,” *Phys. Rev. Lett.*, vol. 78, p. 1207, 1997.
- [14] S. Flach, “Breathers on lattices with long range interaction,” *Phys. Rev. E*, vol. 58, p. R4116, 1998.
- [15] S. Flach, K. Kladko, and S. Takeno, “Acoustic breathers in two-dimensional lattices,” *Phys. Rev. Lett.*, vol. 79, p. 4838, 1997.
- [16] A.E. Miroschnichenko, S. Flach, and Y.S. Kivshar, “Fano resonances in nanoscale structures,” *Rev. Mod. Phys.*, vol. 82, p. 2257, 2010.
- [17] S. Flach, A.E. Miroschnichenko, V. Fleurov, and M.V. Fistul, “Fano resonances with discrete breathers,” *Phys. Rev. Lett.*, vol. 90, p. 084101, 2003.
- [18] U. Fano, “Effects of configuration interaction on intensities and phase shifts,” *Phys. Rev.*, vol. 124, p. 1866, 1961.